

Self-induced path formation among local attractors and spatiotemporal chaos in a complex Ginzburg-Landau equation

Kenju Otsuka

NTT Basic Research Laboratories, Musashino-shi, Tokyo 180, Japan

(Received 11 December 1990)

Spatiotemporal behaviors involving coexisting attractors are investigated in discrete complex time-dependent Ginzburg-Landau equation systems. Complex dynamics connecting local attractors and an "attractor complex" born from destabilized coexisting equilibria are studied through numerical simulations. Majority-rule-based switching among two surviving attractors, inherent unstable motions reflecting the nature of the attractor complex, and "history-dependent" path formation resulting in the recovery of memory are shown in weakly coupled regimes. A relation with a continuum limit is briefly discussed.

Spatiotemporal behavior of spatially coupled nonlinear systems far from thermal equilibrium is a crucial problem in complex dynamics. In general, different equilibria (spatial structures) coexist in the stationary state in high-dimensional systems. The complex time-dependent Ginzburg-Landau (CTDGL) equation [1,2], which describes turbulent phenomena in spatially coupled nonlinear oscillator systems, is a good example for investigating the interplay between coexisting attractors. We investigate CTDGL systems in a small-system-size limit, paying special attention to dynamics involving multiple attractors, and show how dynamics change when the system size increases and the equation approaches the continuum limit [1,2].

Consider a CTDGL system with complex coefficients [3], assuming $\hat{\Psi}_i = \tilde{\Psi}_i \exp(j\omega t)$ (ω is the natural frequency and $j = \sqrt{-1}$), then

$$\begin{aligned} \dot{\tilde{\Psi}}_i = & \mu_i \tilde{\Psi}_i + (\alpha_1 + j\alpha_2)(\tilde{\Psi}_{i+1} + \tilde{\Psi}_{i-1} - 2\tilde{\Psi}_i) \\ & - (1 - j\beta)|\tilde{\Psi}_i|^2 \tilde{\Psi}_i, \quad i = 1, 2, \dots, N \end{aligned} \quad (1)$$

in which we employ the periodic boundary condition, i.e., $\tilde{\Psi}_{N+1} = \tilde{\Psi}_1$, where we can set $\tilde{\Psi}_i = \Psi_i \exp(j\phi_i)$ (Ψ_i is the amplitude and ϕ_i the phase).

With locking conditions, the steady-state solutions given by

$$\begin{aligned} \bar{\Psi}_{i+1}^l = \bar{\Psi}_i^l = & \{ \mu + 2\alpha_1 [\cos(\Delta\bar{\phi}_i^l) - 1] \}^{1/2}, \\ \Delta\bar{\phi}_i^l \equiv & (\phi_{i+1} - \phi_i)^l = 2\pi l / N, \end{aligned}$$

and

$$\Omega^l = \omega - (2\alpha_2 - \beta \bar{\Psi}_i^2) + 2\alpha_2 \cos(\Delta\bar{\phi}_i^l),$$

in which $l = 0, 1, \dots, N-1$, are deduced as equilibria.

First, let us consider briefly the simplest case of $N=3$, which will provide a base for larger system sizes. When the on-site nonlinearity β is increased from zero, a symmetric steady-state σ^0 (i.e., in-phase locking state) that is stable in time is realized at first. When β increases above the first threshold $\beta_{th,1}$, the σ^0 state (node) becomes unstable and a stable asymmetric steady state (focus), i.e.,

$\sigma_{(l=1)}^+$ or $\sigma_{(l=2)}^-$ is realized, depending on initial conditions (symmetry breaking). As β increases further, the asymmetric steady state becomes dynamically unstable and period doubles to asymmetric chaos, featuring a Shil'nikov-type [4] reinjection motion toward σ^\pm via the saddle σ^s , in which one of the relative phases equals zero, and an intersaddle motion [5]. As β increases up to $\beta_{th,2}$, a symmetry-recovering crisis takes place and heteroclinic chaos connecting the two homoclinic attractors via σ^s appears.

Next, let us consider the dynamics when the system size N is increased. The bifurcation scenario is as follows. As the on-site nonlinearity β is increased from zero, the σ^0 state is realized stably in time up to the first threshold $\beta_{th,1}$. In the region just above $\beta_{th,1}$, spatiotemporal chaos (STC) reflecting unstable motions around a basin boundary σ^s state, which is not captured by any particular local attractor, appears for quite a while, as will be discussed later. Hereafter, we call this instability global STC. As β is increased beyond this region, two states $l=(N-1)/2$ (i.e., σ^+) and $l=(N+1)/2$ (σ^-) survive, whereas other solutions become unstable foci for *odd* N [6]. For *even* N , only the $l=N/2$ (σ^π) attractor survives. The present bifurcation scenario generally exists in weakly coupled regimes independently of the system size N . A bifurcation diagram for $N=5$ is shown in Fig. 1, where $\mu=1$ and $\alpha_1=\alpha_2 \equiv \alpha=0.1$ are assumed. Above the first threshold $\beta_{th,1}$, one of the above two states is realized stably, depending on initial conditions (symmetry breaking) and exhibits Hopf bifurcation leading to asymmetrical local chaos. As β is increased up to the second threshold, cooperative switching among the two attractors takes place via the σ^s state. As α (and/or N) is increased, $\beta_{th,2}$ rapidly approaches $\beta_{th,1}$ and at the same time the above-mentioned global STC region spreads.

Now let us consider the σ^s state for $N > 3$. The σ^s state, where one of the relative phases $\Delta\phi_i(t)$ equals zero, dramatically changes its nature and exhibits *synchronized* unstable motions such that $\tilde{\Psi}_1(t) = \tilde{\Psi}_N(t)$, $\tilde{\Psi}_2(t) = \tilde{\Psi}_{N-1}(t)$, $\tilde{\Psi}_3(t) = \tilde{\Psi}_{N-2}(t)$, etc., as N increases. The σ^s state for $N=5$ is shown in Fig. 2(a), where

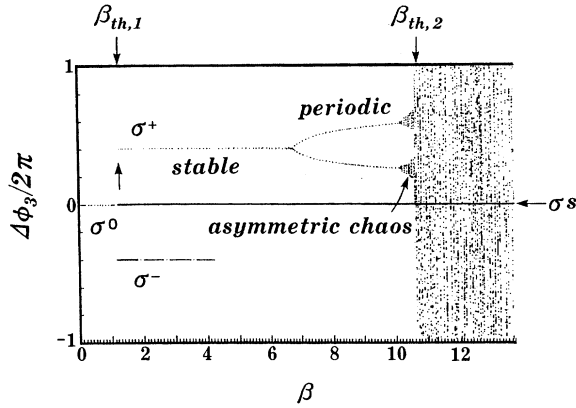


FIG. 1. Bifurcation diagram for a CTDGL system. $N=5$, $\mu=1$, $\alpha=0.1$. Above $\beta_{th,1}$, only the σ^+ state is depicted. For a given on-site nonlinearity β , an initial condition is chosen and successive maxima and minima of $\Delta\phi_3(t)$ are plotted after omitting transients.

$\Delta\phi_2(t)=0$, other relative phases satisfy $\Delta\phi_4(t)=-\Delta\phi_5(t)$ and $\Delta\phi_3(t)=-\Delta\phi_1(t)$. When the σ^s state is excited, two of the relative phases, i.e., $\Delta\phi_1(t)$ and $\Delta\phi_3(t)$, rapidly separate symmetrically. This results from the fact that the two phases $\phi_1(t)$ and $\phi_2(t)$ are synchronized and rotate more rapidly than other phases $\phi_3(t)=\phi_5(t)$ and $\phi_4(t)$. This implies that the intensity of two adjacent ele-

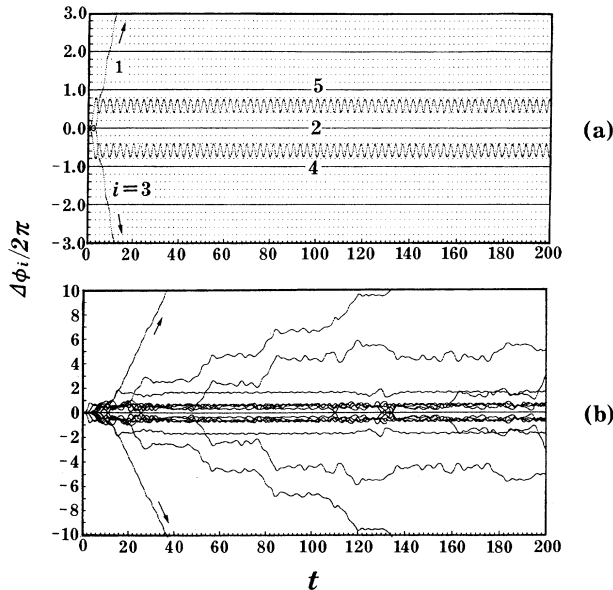


FIG. 2. Unstable motion of basin boundaries σ^s . $\mu=1$, $\alpha=0.1$, and $\beta=11$. (a) $N=5$, (b) $N=19$. These motions do not depend on the on-site nonlinearity β if N and α are fixed. The σ^s state can be easily obtained by setting initial phases symmetrically except for one. (For even N , similar synchronized states are obtained by setting all the initial phases symmetrically such that $\phi_1=\phi_N, \phi_2=\phi_{N-1}, \dots, \phi_{N/2}=\phi_{N/2+1}$).

ments is increased and the phase rotation speed of these elements is increased accordingly as a result of on-site nonlinearity β . In short, pair-phase “rotors” are created.

Here, it should be noted that the averaged value of $\Delta\phi_4 < -\pi$ belongs to the σ^+ attractor and that of $\Delta\phi_5 > \pi$ belongs to the σ^- attractor. If one applies an extremely weak symmetry-breaking noise to this “hybrid” state, one of the two attractors can be excited in the asymmetric chaos regimes. Therefore, this state definitely forms a basin boundary between the two chaotic attractors, similarly to the case of $N=3$.

When N is increased further, the σ^s state exhibits quasiperiodic (torus) and even chaotic motion. (The chaotic σ^s state appears when $N \geq 17$ for $\alpha=0.1$.) The σ^s state exists independently of the system size. This hybrid nature, where one relative phase equals 0, $(N-3)/2$ of relative phases belong to the basin of one attractor ($> \pi$), and the rest $(N-3)/2$ belong to the other attractor basin ($< -\pi$), remains in the regimes in which the σ^s state does not exhibit well-developed chaos. For $\alpha=0.1$, such

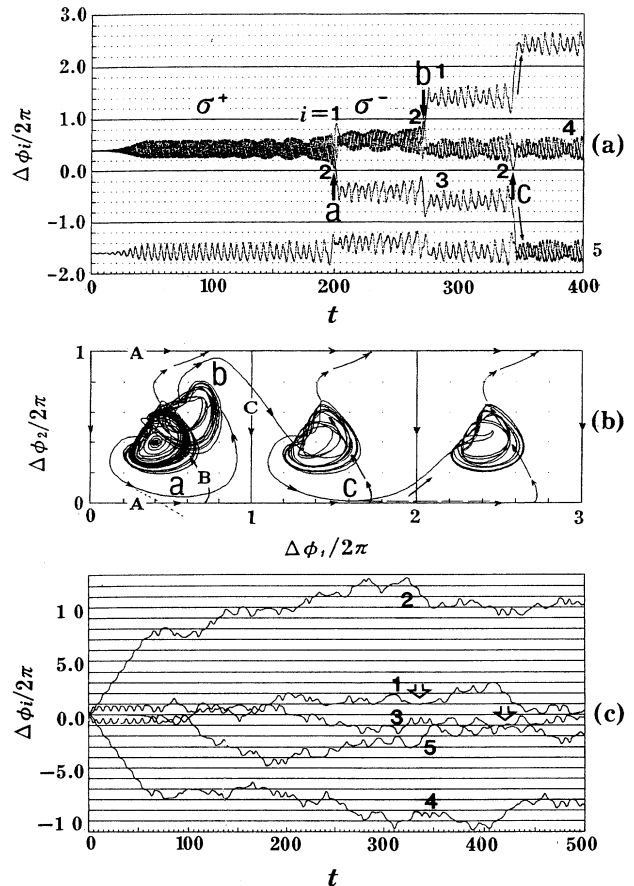


FIG. 3. Relative phase dynamics in $N=5$ CTDGL systems. $\mu=1$. (a) Majority-rule-based switching among σ^\pm attractors. $\alpha=0.1$ and $\beta=10.5$ (b) Corresponding phase-space trajectory projected on $[\Delta\phi_1, \Delta\phi_2]$. Three σ^s motions **A**, **B**, and **C** projected on this plane are also shown. (c) Global STC around the σ^s state. $\alpha=0.15$ and $\beta=2$.

a well-developed chaotic σ^s appears roughly above $N=19$. The σ^s motion for $N=19$ is shown in Fig. 2(b). When the coupling α is increased, the well-developed chaotic σ^s state appears for a smaller N . Inherent unstable motions near basin boundaries may presumably be created by reflecting the unstable character of destabilized coexisting equilibria (namely, the *attractor complex*) above the first threshold and provide a possible origin of the previous global STC. Needless to say, there are N equivalent σ^s states. A similar synchronized chaotic motion also appears for *even* N .

An example for $N=5$ above the second threshold $\beta_{th,2}$ is shown in Fig. 3(a). It should be noted that successful cooperative switching among the two attractors is established when the majority rule is satisfied (see points *a* and *b*), while switching fails when the condition is not met (see point *c*). In short, successful switching occurs when the majority of relative phases cross over the $\sin \Delta\phi_i=0$ line and fall into the basin of attraction of the new attractor just after one relative phase crosses over $\pm 2n\pi$. (At point *a*, for example, just after $\Delta\phi_3$ crosses over zero, $\Delta\phi_{1,4}$ and $\Delta\phi_5$ cross over π and $-2\pi+\pi$, respectively.) When the majority condition is satisfied, the system can switch to the new attractor more easily so as to fulfill the periodic boundary condition. The corresponding phase-space trajectory projected onto $[\Delta\phi_1, \Delta\phi_2]$ is shown in Fig. 3(b). Switching among the two attractors is clearly seen. The *majority-rule-based* cooperative switching between the two attractors has been found to arise independently of system size if N (=odd) is not so large that “information” can spread over the whole system bidirectionally in a time scale which is shorter than the fluctuation period $\propto 1/\alpha \gg N$.

Let us examine the switching process more precisely. At points *a* and *b*, $\Delta\phi_2$ approaches zero and 2π , respectively, and the $i=1$ and 2 elements tend to be locked. As a result, the intensities of the two elements are increased, just as in mutual injection locking in lasers, and pair “rotors” are created transiently. When such appropriate pair rotors are created, $\Delta\phi_{1,3}$ separate, the majority condition for switching is satisfied, and switching is established by crossing over the basin boundary successfully. To be more specific, as can be seen in Fig. 3(b), the system approaches the σ^s state **A** in which $\Delta\phi_2=0$ at point *a*, by creating pair rotors. Then, the system is repelled by **A** and successfully crosses over the basin boundary corresponding to σ^s state **B** with $\Delta\phi_3=0$. At point *b*, after being repelled by σ^s state **A**, the system switches back to the σ^+ attractor by crossing over σ^s state **C** with $\Delta\phi_1=0$. In some cases, the system switches to the other attractor by crossing over the basin boundary directly, like the dotted curve shown in the figure.

At point *c*, $\Delta\phi_{3,1}$ separate when $\Delta\phi_2 \rightarrow 0$ (i.e., σ^s state **A**). In this case, however, the pair rotors are so strong that these two relative phases again cross -2π and 4π successively [see Fig. 3(a)], and the system returns to the basin of attraction of σ^+ as shown in Fig. 3(b). In some cases, longer-lived pair rotors are created and the system approaches the σ^s state asymptotically, like a dashed curve shown in the figure. At this moment, a similar hybrid state featuring the attractor complex motion is excit-

ed. In short, in this approach toward the σ^s state (i.e., one relative phase approaching 0) shown in Fig. 2(a), two separating relative phases periodically cross nearly equivalent relative phase values corresponding to the initial attractor, another relative phase remains within the initial attractor, and the rest approach the value belonging to the other attractor. This implies that the majority of relative phases falls into the basin of the initial attractor almost periodically. This history-dependent motion may return the system to the initial attractor via a path which is periodically opened [see Fig 3(b)] and the initial memory (attractor) is recovered before complete memory blackout, i.e., before the complete hybrid state σ^s is established. (At point *c* of Fig. 3, the system returns to the initial attractor via a path opened at the *first* cycle, i.e., just after $\Delta\phi_1$ crosses over 4π .) The probability for realizing perfect σ^s -type locking during the course of temporal evolution is extremely low in weakly coupled regimes. Consequently, this memory-recovering path is always established in the regime where the σ^s does not exhibit well-developed chaos. Which path (*a*, *b*, or *c*) is formed critically depends on how two adjacent-element phases approach, i.e., on the property of pair rotors.

The symmetrical relative-phase separation also occurs due to random creation of single-phase rotors during the course of temporal evolution [6]. In such a case, however, the system excites another attractor complex instead. Similarly to the *c* motion, the system always returns to the initial attractor. In the case of single rotor, for example, two *adjacent* relative phases separate symmetrically, one relative phase tends to fluctuate around $\pm 2n\pi + \pi$ (n is an integer), $(N-3)/2$ of relative phases remain within the basin of an initial attractor, and the rest approach the other attractor basin. In this process, the system always returns to the initial attractor via a path periodically opened similarly to the case of pair rotors.

As the system size N or the coupling α is increased, the basin of attraction of the surviving attractors is drastically decreased. Consequently, dwell times within the local attractors decrease and switching fails more often because of frequent rotor creation. Furthermore, the previously mentioned global STC develops when switching fails. In short, in these regimes two attractors tend to exist just as small “islands” in a high-dimensional chaotic sea. Finally, the surviving attractors σ^\pm are destroyed, thus leading to the persistent global STC. An example of the persistent global STC around the σ^s state is shown in Fig. 3(c) when α is increased to 0.15, assuming $\mu=1$, $N=5$, and $\beta=2$ and setting initial phases near the σ^s . During the course of temporal evolution, the σ^s -type locking is also attained for a while as indicated by arrows. The global STC also occurs for *even* N when the σ^π attractor is destroyed.

For double limits of strong coupling and large system size (i.e., $N \gg \alpha \approx 1$), which might correspond to a well-studied continuum CTDGL limit, the dynamics change substantially. The σ^0 state survives, with other attractors being dead, and global STC above $\beta_{th,1}$ tends to be dominated by unstable motions around the σ^0 state as one increases $N(\alpha)$, regardless of whether N is even or odd. Finally, intermittent turbulence around the σ^0 state, featur-

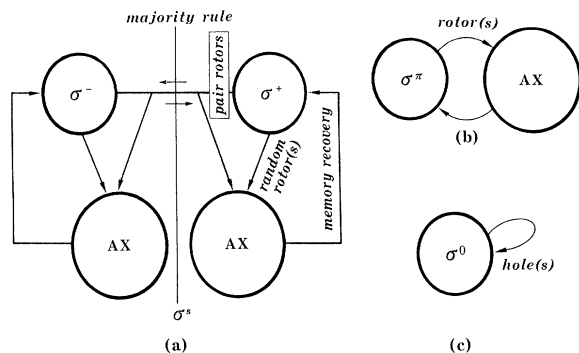


FIG. 4. Conceptual model of self-induced path formation in CTDGL systems, where AX denotes the attractor complex. (a) N =odd; weakly coupled regimes. (b) N =even; weakly coupled regimes. (c) Strongly coupled and large-system regimes.

ing discontinuity phase jumping of $\pm 2n\pi$ (n is an integer), takes place. This phase jump occurs when Ψ_i of a particular element approaches zero (singular point). At the same time, the phase rotation of this element decreases and a trajectory of $\dot{\Psi}_i$ approaches the origin at the discontinuous point [6]. This is nothing more than

the so-called "hole" solution observed in the standard continuum CTDGL equation [2].

On the basis of the computer experiments described so far, the conceptual model of self-induced path formation shown in Fig. 4 is conjectured for CTDGL systems. In weakly coupled regimes, a path connecting each attractor (σ^+ or σ^-) and the attractor complex to which it belongs is created for odd $N \geq 5$ [see Fig. 4(a)], whereas the two homoclinic attractors are simply connected through the saddle for $N=3$. Switching among the two attractors is governed by the majority rule. Which path is formed depends critically on the character of the phase rotors. Various unstable orbits (attractor complex), which succeed the initial attractor nature, are excited according to the number and property of the phase rotors as well. For even N , only the path connecting the σ^π attractor and the attractor complex is formed. [See Fig. 4(b).] When one increases N and/or α , the basin of attraction of surviving attractors decreases thus leading to the global STC featuring attractor complex motions. Finally, in a strongly coupled large system limit [Fig. 4(c)], the intermittent turbulence around the σ^0 state takes place as a result of hole creations, regardless of whether N is even or odd.

The author is indebted to K. Ikeda for suggesting CTDGL problems and for fruitful discussions.

[1] See, for example, Y. Kuramoto, *Chemical Oscillations, Waves, and Turbulence*, edited by H. Haken (Springer-Verlag, Berlin, 1984).

[2] H. Sakaguchi, *Prog. Theor. Phys.* **80**, 743 (1980).

[3] One realistic example which obeys CTDGL dynamics is a coupled detuned class-A laser, e.g., a gas or dye laser in which population and polarization dynamics can be adiabatically eliminated. In this case, one can set $\mu_i=0$ and replace the last term in Eq. (1) by $1/2[(P_i - P_{th})/|\dot{\Psi}_i|^2 - 1/\tau_p](1 - j\beta)\dot{\Psi}_i$ ($\dot{\Psi}_i$, slowly varying complex field; P , pump power; P_{th} , threshold pump

power; τ_p , photon number). Such modifications do not essentially change CTDGL dynamics in weakly coupled regimes.

[4] L.P. Shil'nikov, *Dokl. Akad. Nauk SSSR* **160**, 558 (1965).

[5] K. Otsuka, *Int. J. Mod. Phys. B* (to be published).

[6] K. Otsuka and K. Ikeda, in *Proceedings of Optical Society of America Topical Meeting on Nonlinear Dynamics in Optical Systems*, Afton, 1990, edited by N. Abraham, E. Garmaire, and P. Mandel (Optical Society of America, Washington, D.C., 1991).